

Exploring Micromagnetorotation in Maxwell Viscous Fluid Flow Within a Porous Cylinder

Yolanda Norasia¹, Mohammad Ghani^{2*}

¹ Department of Mathematics, Faculty of Science and Technology, State Islamic University of Walisongo, Semarang 50185, Indonesia

² Data Science Technology, Faculty of Advanced Technology and Multidiscipline, Airlangga University, Surabaya 60115, Indonesia

Corresponding Author Email: mohammad.ghani@fmm.unair.ac.id

Copyright: ©2023 IETA. This article is published by IETA and is licensed under the CC BY 4.0 license (<http://creativecommons.org/licenses/by/4.0/>).

<https://doi.org/10.18280/mmep.100620>

ABSTRACT

Received: 12 April 2023

Revised: 22 August 2023

Accepted: 10 September 2023

Available online: 21 December 2023

Keywords:

Maxwell Fluid, viscous, magnetomicrorotation, Gauss-Seidel method, Stuart number, Prandtl number, material parameter, porosity parameter

The study of viscous fluids, ubiquitous in various industrial engineering applications, frequently reveals intriguing physical phenomena. Among these, micromagnetorotation, the rotation of a viscous fluid under the influence of a magnetic field, has recently garnered significant interest. This research aims to examine the behaviour of micromagnetorotational fluid flow within a porous cylinder. Fundamental equations constituting this analysis include the continuity equation, the momentum equation, and the energy equation, leading to a system of nonlinear ordinary differential equations. These equations are then dimensionally transformed and solved using the Gauss-Seidel numerical scheme under a suitable solution assumption. The investigation focuses on parameters influencing the velocity and temperature profiles of the micromagnetorotational fluid flow, namely viscosity, the Stuart number, the Prandtl number, the material parameter, and porosity. The study reveals that modifications in any of these parameters lead to a decrease in the velocity profile. Conversely, increases in the temperature profile are observed when influenced by the viscosity parameter, the Stuart number, the material parameter, and the porosity parameter. This research is anticipated to offer valuable insights for optimizing fluid flow velocity and temperature within engineering and industrial applications.

1. INTRODUCTION

Fluid dynamics, an applied science that employs mathematical modeling coupled with numerical solution techniques, plays a vital role in engineering and industry. Fundamental to this field are three governing laws: the conservation of mass, Newton's Second Law, and the First Law of Thermodynamics. Fluids are typically classified as either non-viscous or viscous based on their frictional properties, the latter term describing fluids with interparticle friction [1]. Abel's study highlighted how the temperature profiles of fluids could be influenced by viscosity, with an increase in viscosity being associated with a rise in temperature [2]. Ali et al. [3] further explored the impact of magnetic parameters on free convection Magnetohydrodynamic (MHD) viscous fluid flow, finding that a reduction in the value of magnetic parameters led to an increase in the velocity profile. In a yawed cylinder, a significant decrease in temperature profiles was observed with mixed convection [4].

Maxwell Fluids, characterized by their motion under a magnetic field, have been the subject of various investigations. Farooq et al. [5] examined the impact of volumetric concentrations on Maxwell Fluids, noting that increases in the Hartman number, Brownian motion parameter, and Deborah

number led to increased volumetric concentrations. Other studies have indicated that Darcy numbers, Brownian motion parameters, and Eckert numbers influence the flow of Maxwell Fluid across stretching surfaces [6]. Intriguingly, the presence of a magnetic field parameter was found to contribute to a decline in fluid velocity [7]. Further research showed that magnetic particles could influence the velocity and temperature distribution of the fluid [8]. Krishna and Chamkha [9] extended this work, examining the flow of viscous and magnetic parameters through a porous medium, and noted that an increase in magnetic and viscous parameters led to a decrease in system speed.

Besides the magnetic effects, microrotation also impacts the movement of viscous fluids. Fluid particles undergo microrotation due to friction, a phenomenon explored by Fatunmbi and Adeniyani [10]. Their study on heat and mass transfer in MHD micropolar fluid over a stretching sheet showed that an increase in material parameters led to a decrease in temperature and concentration profiles [10]. Further MHD studies on micropolar fluids passing by a stretching surface revealed an increase in velocity, but a decrease in temperature and concentration fields with the swelling of the primary slip parameter values [11]. Numerical analysis of micropolar fluid flow through stretchable surfaces indicated that the heat transfer rate decreases as the heat source value parameter

increases [12]. Aslani et al. [13] discovered that when MHD micropolar flow is connected to magnetizing fluid, micromagnetorotation can potentially increase fluid flow velocity. However, the presence of micromagnetorotation was found to decrease fluid velocity and microrotation profile [14], in addition to suppressing convection and reducing heat transfer with Hartmann parameters [14]. Micromagnetorotation refers to the micromotion of externally applied magnetic fluid particles, resulting in thinner velocity boundary layers [15].

This study aims to combine two fluid characteristics, viscosity and micromagnetorotation, to analyze the velocity and temperature of fluid influenced by several parameters: viscosity, the Stuart number, the Prandtl number, material, and porosity. Few studies have employed these parameters collectively in a micromagnetorotational fluid flow model. Fluids exhibiting micromagnetorotation characteristics are found in colloidal suspensions, cooling systems, and numerous other applications [15]. By integrating viscous and micromagnetorotation characteristics, this research seeks to analyze fluid velocity and temperature within a porous cylinder medium using the aforementioned parameters. The equations governing this study, derived from the Laws of Physics, include the continuity equation, momentum equation, and energy equation, which are solved with a MATLAB-assisted numerical solution. With the influence of viscosity, the Stuart number, the Prandtl number, material, and porosity parameters, this research may provide valuable insights for optimizing fluid velocity and temperature in engineering and industrial applications.

2. PROBLEM FORMULATION

In the case of a maxwell-viscous fluid passing through a porous cylinder, three equations can be derived, namely the continuity equation, momentum equation, and energy equation as follows.

(1) Continuity equation

$$\frac{\partial \bar{u}}{\partial \bar{x}} + \frac{\partial \bar{v}}{\partial \bar{y}} = 0 \quad (1)$$

(2) Momentum equation

$$\begin{aligned} \bar{u} \frac{\partial \bar{u}}{\partial \bar{x}} + \bar{v} \frac{\partial \bar{u}}{\partial \bar{y}} = & -\frac{\partial \bar{p}}{\partial \bar{x}} + \nu \left(\frac{\partial^2 \bar{u}}{\partial \bar{y}^2} \right) \\ & - \frac{1}{\rho} \sigma (B_0)^2 (\bar{u} - \bar{u}_e) + (\bar{T} - \overline{(T)}_\infty) g_{\bar{x}} \\ & - \frac{k_0}{\rho} \left(\bar{u} \frac{\partial^3 \bar{u}}{\partial \bar{x} \partial \bar{y}^2} + \bar{v} \frac{\partial^3 \bar{u}}{\partial \bar{y}^3} - \right. \\ & \left. \frac{\partial \bar{u}}{\partial \bar{y}} \frac{\partial^2 \bar{u}}{\partial \bar{x} \partial \bar{y}} + \frac{\partial \bar{u}}{\partial \bar{x}} \frac{\partial^2 \bar{u}}{\partial \bar{y}^2} + \frac{\partial \bar{N}}{\partial \bar{y}} \right) \end{aligned} \quad (2)$$

(3) Energy equation

$$\bar{u} \frac{\partial \bar{T}}{\partial \bar{x}} + \bar{v} \frac{\partial \bar{T}}{\partial \bar{y}} = \alpha_{mv} \frac{\partial^2 \bar{T}}{\partial \bar{y}^2} + Q_0 (\bar{T} - \overline{(T)}_\infty) \quad (3)$$

The dimensional boundary conditions are as follows:

$$\begin{aligned} \bar{u} = \bar{v} = 0, \bar{N} = -n \frac{\partial \bar{u}}{\partial \bar{y}}, \bar{T} = T_w \text{ for } \bar{y} = 0 \\ \bar{u} = \bar{u}_e, \bar{u} = \bar{v}, \bar{N} = 0, \bar{T} = T_\infty \text{ for } \bar{y} \rightarrow \infty \end{aligned}$$

The following equations can be converted into non-dimensional governing equations by substituting non-dimensional variables [16, 17].

$$x = \frac{\bar{x}}{a}; y = Re^{\frac{1}{2}} \frac{\bar{y}}{a}; u = \frac{\bar{u}}{U_\infty}; v = Re^{\frac{1}{2}} \frac{\bar{v}}{U_\infty};$$

$$T = \frac{\bar{T} - T_\infty}{T_w - T_\infty}; p = \frac{\bar{p}}{\rho U_\infty^2};$$

$$u_e(x) = \frac{\bar{u}_e(x)}{U_\infty}; g_x = -g \sin\left(\frac{\bar{x}}{a}\right)$$

and non-dimensional parameters defined as follows [18, 19].

$$Pr = \frac{\nu}{\alpha_{mv}}; Gr = \frac{g \beta (T_w - T_\infty) a^3}{\nu^3};$$

$$V_s = \frac{k_0 U_\infty}{a \rho \nu}$$

$$K = \frac{k_0}{\mu}; Re = \frac{U_\infty a}{\nu}; \lambda = \frac{Gr}{Re^2}$$

$$St = \frac{\sigma B^2 a}{\rho U_\infty};$$

$$Q = \frac{a^2 Q_0}{(g(T_w - T_\infty) \beta)^{\frac{1}{2}} (\rho c_p)}$$

$$\phi = \frac{\nu}{K} \frac{a}{U_\infty}$$

The following non-dimensional equations can be obtained by substituting non-dimensional variables and parameters in the governing equation in Eqs. (1)-(3).

(1) Continuity equation

$$\frac{\partial u}{\partial x} + \frac{\partial v}{\partial y} = 0 \quad (4)$$

(2) Momentum equation

$$u \frac{\partial u}{\partial x} + v \frac{\partial u}{\partial y} = -\frac{\partial p}{\partial x} + \frac{\partial^2 u}{\partial y^2} - (St + \phi)(u - u_e) + \lambda \theta \sin x + K \frac{\partial N}{\partial y} - V_s \left(\frac{\partial}{\partial x} \left(u \frac{\partial^2 u}{\partial y^2} \right) + v \frac{\partial^3 u}{\partial y^3} - \frac{\partial u}{\partial y} \frac{\partial^2 u}{\partial x \partial y} \right) \quad (5)$$

(3) Energy equation

$$u \frac{\partial T}{\partial x} + v \frac{\partial T}{\partial y} = \frac{1}{Pr} \frac{\partial^2 T}{\partial y^2} + QT \quad (6)$$

by using non-dimensional variable, non-dimensional boundary conditions are as follows:

$$u = v = 0, N = -n \frac{\partial u}{\partial y}, T = 1 \text{ for } y = 0$$

$$u = u_e, N = 0, T = 0 \text{ for } y \rightarrow \infty$$

In this study, there were two velocity components, so we used stream function to connect them as follows [20]:

$$u = \frac{\partial \psi}{\partial y}; v = -\frac{\partial \psi}{\partial x}$$

Substituting the stream function in Eqs. (4)-(6), then we get

(1) Continuity equation

$$\frac{\partial \psi}{\partial x \partial y} = \frac{\partial \psi}{\partial x \partial y} \quad (7)$$

(2) Momentum equation

$$\frac{\partial \psi}{\partial y} \left(\frac{\partial^2 \psi}{\partial x \partial y} \right) - \frac{\partial \psi}{\partial y} \left(\frac{\partial^2 \psi}{\partial y^2} \right) = u_e \frac{\partial u_e}{\partial x} + \frac{\partial^3 \psi}{\partial y^3}$$

$$-(St + \phi) \left(\frac{\partial \psi}{\partial y} - u_e \right) + \lambda \theta \sin x + K \frac{\partial N}{\partial y}$$

$$-V_s \left(\frac{\partial}{\partial x} \left(\frac{\partial \psi}{\partial y} \left(\frac{\partial^3 \psi}{\partial y^3} \right) \right) + \frac{\partial \psi}{\partial y} \frac{\partial^4 \psi}{\partial y^4} - \frac{\partial^2 \psi}{\partial y^2} \frac{\partial^3 \psi}{\partial x \partial y^2} \right) \quad (8)$$

(3) Energy equation

$$\frac{\partial \psi}{\partial y} \frac{\partial T}{\partial x} + \frac{\partial \psi}{\partial x} \frac{\partial T}{\partial y} = \frac{1}{Pr} \frac{\partial^2 T}{\partial y^2} + QT \quad (9)$$

Then the similarity variables are substituted in Eqs. (7)-(9),

so that the similarity equation is obtained as follows.

$$\frac{\partial^3 f}{\partial y^3} + f \frac{\partial^2 f}{\partial y^2} - \left(\frac{\partial f}{\partial y} \right)^2 + 1 + \lambda T - (St + \phi) \left(\frac{\partial f}{\partial y} - \frac{\sin x}{x} \right) + K \frac{\partial h}{\partial y} - V_s \left(2 \frac{\partial f}{\partial y} \frac{\partial^3 f}{\partial y^3} - f \frac{\partial^4 u}{\partial y^4} - \left(\frac{\partial^2 f}{\partial y^2} \right)^2 \right) = 0 \quad (10)$$

$$\frac{1}{Pr} \frac{\partial^2 T}{\partial y^2} + f \frac{\partial T}{\partial y} + QT = 0 \quad (11)$$

The boundary conditions are as follows:

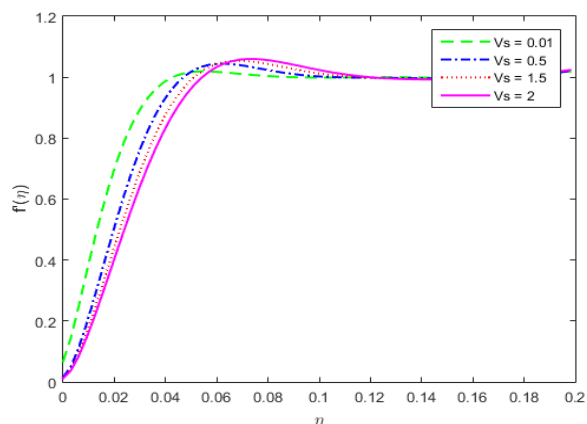
$$f = \frac{\partial f}{\partial \eta} = 0, h = -n \frac{\partial^2 f}{\partial y^2}, T = 1 \text{ for } y = 0$$

$$\frac{\partial f}{\partial y} = 1, h = T = 0 \text{ for } y \rightarrow \infty$$

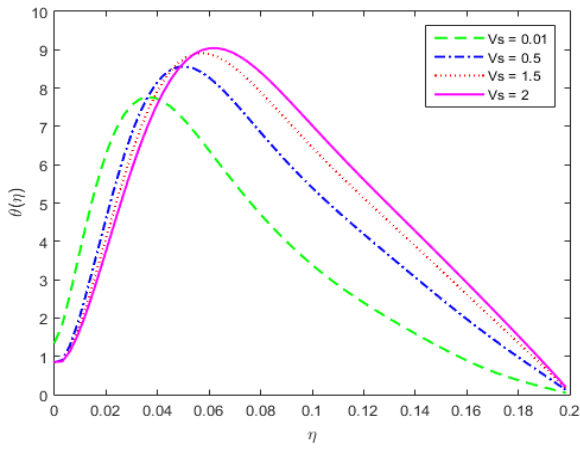
3. RESULT AND DISCUSSION

This study observes the velocity and temperature of the micromagnetorotation maxwell-viscous fluid flow that passes through the cylinder surface with the influence of viscosity parameter, Stuart number, Prandtl number, material parameter, and the porosity parameter. Similarity equations are solved numerically using the Gauss-Seidel method. Numerical results are presented in graphical form in the form of fluid velocity and temperature.

The effect of viscosity with variations of 0.01, 0.5, 1.5, and 2 on the velocity profile in Figure 1(a) shows that the higher the viscosity parameter, the lower the fluid velocity. In contrast to the temperature profile in Figure 1(b), the more the viscosity parameter is increased, the temperature profile also increases. Friction between fluids increases the effect of viscosity on the temperature profile. Fluids with a higher viscosity contain more particles. The number of particles causes the momentum between profile decreases and the temperature profile increases. the particles to increase, consequently, the velocity.

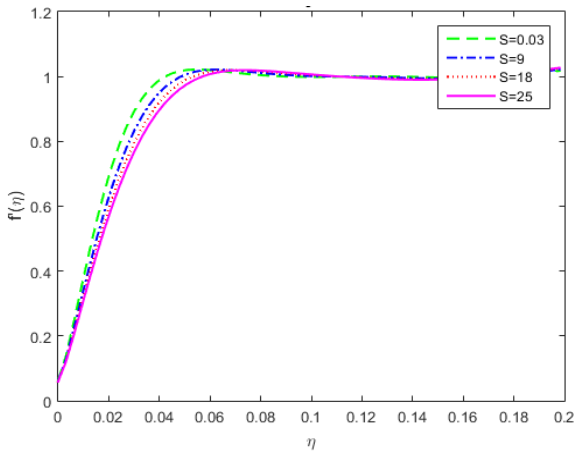


(a) Velocity profile

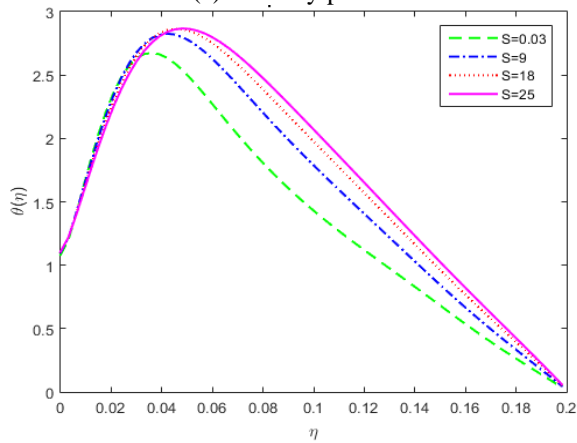


(b) Temperature profile

Figure 1. Variation of viscosity parameters



(a) Velocity profile



(b) Temperature profile

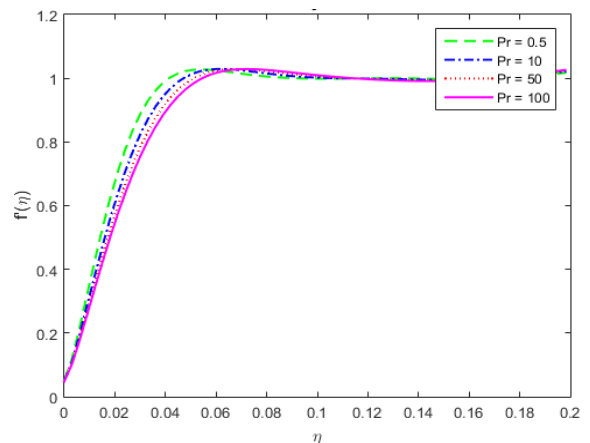
Figure 2. Variation of Stuart number parameters

The variations in the Stuart number parameter for the velocity profile and temperature profile are shown in Figure 2. The Stuart number can be used to describe magnetic interactions in liquids. Stuart number variations used are 0.03, 9, 18, and 25. The larger the Stuart number parameter, it can be seen in Figure 2(a) that the fluid flow velocity decreases. The existence of the Lorentz force on the Stuart number parameter increases the magnetic field that affects the system simultaneously. This is due to the Lorentz force generated by the micro magneto rotation characteristics of the maxwell-viscous fluid. As a result, the micromagnetorotation maxwell-viscous fluid decreases with variations in Stuart number parameters. Figure 2(b) shows that the temperature of the fluid

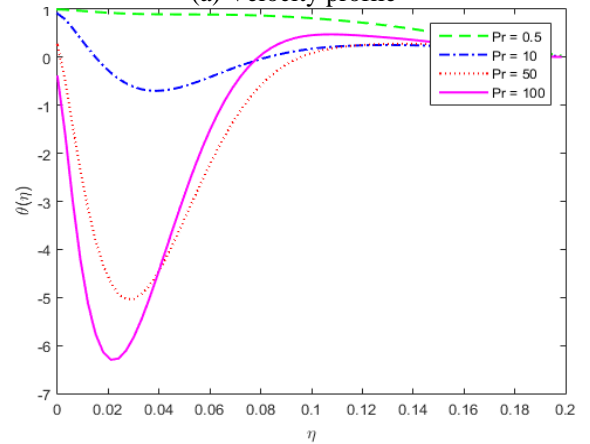
increases when given an increase in the variation of the Stuart number parameter. This is due to the Stuart number parameter being inversely proportional to the density. The greater the variation in the Stuart number, the smaller the density of the fluid so that the temperature in the micromagnetorotation maxwell-viscous fluid increases at every particular η point.

Figure 3 shows variations in the Prandtl number. The Prandtl number is the ratio between kinematic viscosity and thermal diffusion. Variations in the Prandtl number used are 0.5, 10, 50, and 100. The parameter Prandtl number is 10 in water. While in the range of 50 to 100 in oil. Figure 3(a) shows that the greater the variation in the Prandtl number parameters, the fluid velocity decreases. The Prandtl number is directly related to the kinematic viscosity.

Likewise, Figure 3(b) shows that the greater the variation in the Prandtl number parameter, the faster the fluid temperature decreases. Thermal diffusion is inversely proportional to the Prandtl number parameter. As a result, when the Prandtl number parameter is increased, the fluid's temperature distribution decreases.



(a) Velocity profile



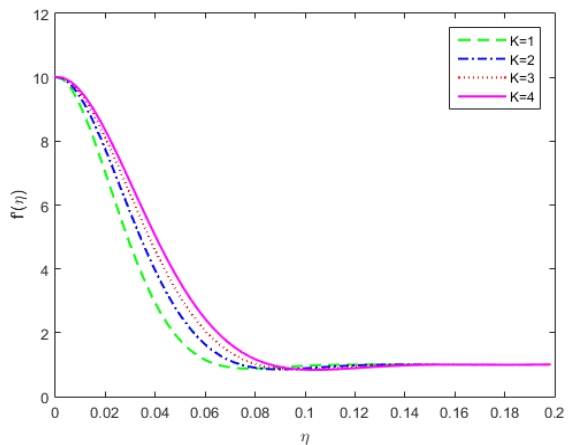
(b) Temperature profile

Figure 3. Variation of Prandtl number parameters

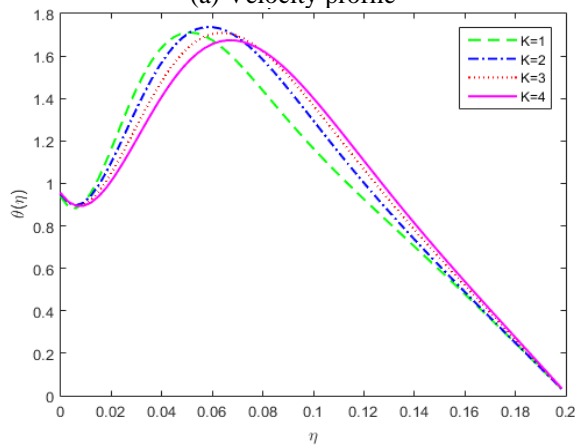
In Figure 4, we can see the variation in material parameters regarding velocity and temperature profiles. Rotational and dynamic viscosities determine the material parameters. Fluids with material parameters $K=0$ are non-viscous fluids [21]. In this study, maxwell-viscous fluid was used with variations in material parameters $K=1,2,3,4$. Figure 4(a) shows that the greater the given material parameters, the fluid velocity will decrease from $\eta=0.1$ to $\eta=0.2$. This is due to the greater friction resulting in greater momentum. Therefore, the velocity of the fluid decreases. Conversely, in Figure 4(b), the greater the

material parameters, the more fluid temperature increases. The existence of friction between particles can generate heat. Thus, the greater the material parameters, the higher the fluid temperature.

The effect of the porosity parameters with variations of 0.01, 0.1, 0.7, and 1.2 on the velocity and temperature profiles are shown in Figure 5. Figure 5(a) shows that the higher the porosity parameter, the lower the fluid velocity. In contrast to the fluid temperature in Figure 5(b), the more the porosity parameter is increased, the fluid temperature also increases. An increase in the porosity parameter results in obstructed fluid movement while the resistance forms friction which generates heat.

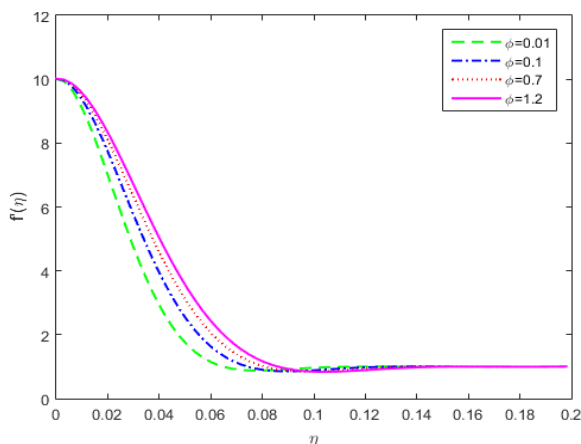


(a) Velocity profile

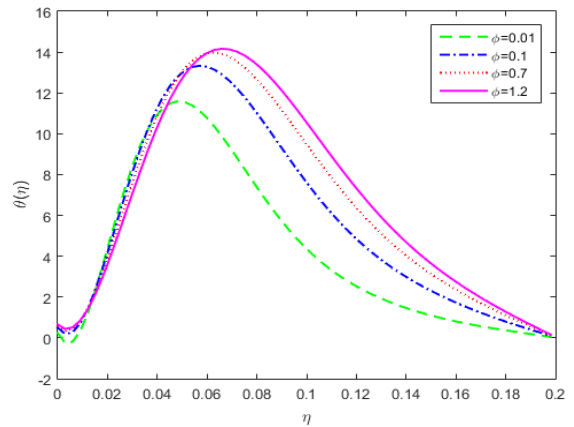


(b) Temperature profile

Figure 4. Variation of material parameters



(a) Velocity profile



(b) Temperature profile

Figure 5. Variation of porosity parameters

From Figure 1 to Figure 5, the velocity profile decreases due to the influence of the five parameters. Temperature is affected by the viscosity parameter, Stuart number, material parameter, and porosity parameter. Optimization of the temperature profile in micromagnetorotation viscous fluid flow can use the increase in the viscosity parameter, Stuart number, material parameter, and porosity parameter. The character of micromagnetorotation involves a magnetic field and microrotational motion in viscous fluids. The results showed the optimal temperature of the micromagnetorotation viscous fluid.

4. CONCLUSIONS

The governing equations for the maxwell-viscous fluid micromagnetorotation passing through a porous cylinder are the equations of continuity, momentum, and energy. These equations are then transformed into dimensionless equations and similarity equations. The final equation obtained is solved numerically using Gauss-Seidel. The parameters that affect the dynamics of the maxwell-viscous fluid are observed. The following is the influence of the viscosity, Stuart number, Prandtl number, material parameter, and porosity parameters.

- (1) The effect of the viscosity parameter causes the velocity profile on the maxwell-viscous fluid to decrease and the temperature profile on the maxwell-viscous fluid to increase.
- (2) The influence of the Stuart number causes the velocity profile of the maxwell-viscous fluid to decrease and the temperature profile to increase.
- (3) The influence of the Prandtl number causes the velocity and temperature profile of the maxwell-viscous fluid to decrease.
- (4) The effect of material parameters causes the velocity profile on the maxwell-viscous fluid to decrease and the temperature profile on the Maxwell-Viscous fluid to increase.
- (5) The influence of the porosity parameter causes the velocity profile on the maxwell-viscous fluid to decrease and the temperature profile on the maxwell-viscous fluid to increase.

Research with the characteristics of micromagnetorotation has not been widely carried out. It is possible to conduct an analysis of the flow microrotation profile in biological applications such as blood circulation by developing a linear and angular momentum model.

FUNDING

This work was funded by the Faculty of Advanced Technology and Multidiscipline, Airlangga University, East Java, Indonesia (Grant No.: 121/UN3.1.17/PT/2022).

REFERENCES

- [1] Jafeer, M.B., Mustafa, M. (2021). A study of elasto-viscous fluid flow by a revolving disk with heat dissipation effects using HAM based package BVPh 2.0. *Scientific Reports*, 11: 4514. <https://doi.org/10.1038/s41598-021-83864-z>
- [2] Abel, M.S., Mahesha, N. (2008). Heat transfer in MHD viscoelastic fluid flow over a stretching sheet with variable thermal conductivity, non-uniform heat source and radiation. *Applied Mathematical Modelling*, 32(10): 1965-1983. <https://doi.org/10.1016/j.apm.2007.06.038>
- [3] Ali, Q., Riaz, S., Awan, A.U. (2020). Free convection MHD flow of viscous fluid by means of damped shear and thermal flux in a vertical circular tube. *Physica Scripta*, 95(9): 095212. <https://doi.org/10.1088/1402-4896/abab39>
- [4] Patil, P.M., Shashikant, A., Roy, S., Hiremath, P.S. (2020). Mixed convection flow past a yawed cylinder. *International Communications in Heat and Mass Transfer*, 114: 104582. <https://doi.org/10.1016/j.icheatmasstransfer.2020.104582>
- [5] Farooq, U., Lu, D., Munir, S., Ramzan, M., Suleman, M., Hussain, S. (2019). MHD flow of Maxwell Fluid with nanomaterials due to an exponentially stretching surface. *Scientific Reports*, 9(1): 7312. <https://doi.org/10.1038/s41598-019-43549-0>
- [6] Dawar, A., Saeed, A., Shah, Z., Kumam, W., Islam, S., Kumam, P. (2021). Analytical simulation for magnetohydrodynamic Maxwell Fluid flow past an exponentially stretching surface with first-order velocity slip condition. *Coatings*, 11(8): 1009. <https://doi.org/10.3390/coatings11081009>
- [7] Loganathan, K., Alessa, N., Namgyel, N., Karthik, T.S. (2021). MHD flow of thermally radiative Maxwell Fluid past a heated stretching sheet with Cattaneo-Christov dual diffusion. *Journal of Mathematics*, 2021: 1-10. <https://doi.org/10.1155/2021/5562667>
- [8] Norasia, Y., Widodo, B., Adzkiya, D. (2021). Pergerakan aliran mhd ag-air melewati bola pejal. *Limits: Journal of Mathematics and Its Applications*, 18(1): 15-21. <http://dx.doi.org/10.12962/limits.v18i1.7888>
- [9] Krishna, M.V., Chamkha, A.J. (2020). Hall and ion slip effects on MHD rotating flow of elasto-viscous fluid through porous medium. *International Communications in Heat and Mass Transfer*, 113: 104494. <https://doi.org/10.1016/j.icheatmasstransfer.2020.104494>
- [10] Fatunmbi, E.O., Adeniyani, A. (2018). Heat and mass transfer in MHD micropolar fluid flow over a stretching sheet with velocity and thermal slip conditions. *Open Journal of Fluid Dynamics*, 8: 195-215.
- [11] Ramadevi, B., Anantha Kumar, K., Sugunamma, V., Ramana Reddy, J.V., Sandeep, N. (2020). Magnetohydrodynamic mixed convective flow of micropolar fluid past a stretching surface using modified Fourier's heat flux model. *Journal of Thermal Analysis and Calorimetry*, 139: 1379-1393. <https://doi.org/10.1007/s10973-019-08477-1>
- [12] Singh, K., Pandey, A.K., Kumar, M. (2021). Numerical solution of micropolar fluid flow via stretchable surface with chemical reaction and melting heat transfer using Keller-Box method. *Propulsion and Power Research*, 10(2): 194-207. <https://doi.org/10.1016/j.jprr.2020.11.006>
- [13] Aslani, K.E., Benos, L., Tzirtzilakis, E., Sarris, I.E. (2020). Micromagnetorotation of MHD micropolar flows. *Symmetry*, 12(1): 148. <https://doi.org/10.3390/sym12010148>
- [14] Aslani, K.E., Sarris, I.E. (2021). Effect of micromagnetorotation on the heat transfer of micropolar Hartmann flow. *Thermal Science and Engineering Progress*, 26: 101129. <https://doi.org/10.1016/j.tsep.2021.101129>
- [15] Khan, M.S., Hameed, I. (2023). A new magneto-micropolar boundary layer model for liquid flows--Effect of micromagnetorotation (MMR). *arXiv preprint arXiv:2308.08457*. <https://doi.org/10.48550/arXiv.2308.08457>
- [16] Alkasasbeh, H.T. (2018). Numerical solution of micropolar Casson fluid behaviour on steady MHD natural convective flow about a solid sphere. *Journal of Advanced Research in Fluid Mechanics and Thermal Sciences*, 50(1): 55-66.
- [17] Al Nuwairan, M., Hafeez, A., Khalid, A., Souayah, B., Alfidhli, N., Alnaghmosh, A. (2022). Flow of Maxwell Fluid with heat transfer through porous medium with thermophoresis particle deposition and Soret-Dufour effects: Numerical solution. *Coatings*, 12(10): 1567. <https://doi.org/10.3390/coatings12101567>
- [18] Ghani, M. (2021). Numerical results of mixed convection flow over a flat plate with the imposed heat and angle of inclination. *Euler: Jurnal Ilmiah Matematika, Sains dan Teknologi*, 9(2): 85-93. <https://doi.org/10.34312/euler.v9i2.11782>
- [19] Reddy, Y.D., Goud, B.S., Nisar, K. S., Alshahrani, B., Mahmoud, M., Park, C. (2023). Heat absorption/generation effect on MHD heat transfer fluid flow along a stretching cylinder with a porous medium. *Alexandria Engineering Journal*, 64: 659-666. <https://doi.org/10.1016/j.aej.2022.08.049>
- [20] Widodo, B., Arif, D.K., Aryany, D., Asiyah, N., Widjajati, F.A., Kamiran, K. (2017). The effect of magnetohydrodynamic nano fluid flow through porous cylinder. *AIP Conference Proceedings*, 1867(1): 020069. <https://doi.org/10.1063/1.4994472>
- [21] Khan, W.A., Rashad, A.M., El-Kabeir, S.M.M., El-Hakiem, A.M.A. (2020). Framing the MHD micropolar-nanofluid flow in natural convection heat transfer over a radiative truncated cone. *Processes*, 8(4): 379. <https://doi.org/10.3390/pr8040379>

NOMENCLATURE

(u, v)	velocity components
S_t	Stuart Number
P_r	Prandtl Number
V_s	viscosity parameter
K	material parameter

ϕ	porosity parameter	ψ	stream function
R_e	Reynolds number	x	streamwise coordinate
G_r	Grashof number	y	transverse coordinate
T	temperature fluid	λ	thermal diffuses
ρ	density of Maxwell-Viscous fluid	ν	kinematic viscosity
g_x	gravitational acceleration	Q	heat-generation
B	Magnetic inducement	Q_0	Volumetric rate of heatsource